Epitope mapping of SARS-CoV 2 RBDs by hydroxyl radical protein footprinting reveals the importance of including negative antibody controls.

Daniel Nyberg Larsen*[+], Jakub Zbigniew Kaczmarek[+], Yaseelan Palarasah[¤], Jonas Heilskov Graversen[¤], Peter Højrup*

* Department of Biochemistry and Molecular Biology, University of Southern Denmark, Campusvej 55, DK-5230 Odense, Denmark

[¤] Department of Cancer and Inflammation, Institute of Molecular Medicine, Faculty of Health and Medical Sciences, University of Southern Denmark, Odense, Denmark.

[+] Ovodan Biotech A/S, Havnegade 36, DK-5000 Odense, Denmark

Keywords: RBD Alpha, RBD Delta, Mass spectrometry, Fenton chemistry, Covid-19

Journal:

Elsevier journal

Abstract

Epitope mapping methods using hydroxyl radical protein footprinting (HRPF) are currently hampered by high initial cost and complex experimental setup. Here we set out to present a generally applicable method using Fenton chemistry for mapping of epitopes and paratopes in a standard laboratory setting. Furthermore, the described method illustrates the importance of controls on several levels when performing mass spectrometry-based epitope mapping. In particular, the inclusion of negative antibody controls has not previously been widely utilized in epitope mapping by HRPF analysis. In order to limit the false positives, we further introduced quantification by TMT labelling, thereby allowing for direct comparison between sample conditions and biological triplicates. Lastly, up to six technical replicates were incorporated in the experimental setup in order to achieve increased depth of the final analysis.

Both binding and openings of regions on receptor binding domain (RBD) from SARS-CoV-2 Spike Protein, Alpha and Delta variants, were observed. The negative control antibody experiment, combined with the high overlap between biological triplicates, resulted in the exclusion of 40% of the significantly changed regions, including both binding and opening regions. The identified binding region agrees with the literature for neutralizing antibodies towards SARS-CoV-2 Spike Protein.

The presented method is an easily implementable technique for the analysis of HRPF in a generic MS-based laboratory. The high reliability of the data was achieved by increasing the number of technical and biological replicates combined with negative antibody controls.

Introduction

In December 2019 a novel coronavirus (SARS-Cov-2) crossed species barriers to infect humans and has effectively been transmitted from person to person [1]. Infection with SARS-Cov-2 causes the coronavirus disease 19 (COVID-19) with influenza like symptoms, ranging from mild disease to server lung injury and multi-organ failure, potentially leading to death for older patients with other co-morbidities [2,3].

SARS-Cov-2 infect the host by a densely glycosylated spike (S) protein [2]. The S protein is a trimeric class I fusion protein that exists in two different conformations and undergoes a substantial structural rearrangement to fuse the viral membrane with the host cell membrane [2]. The fusion is triggered when a subunit of the S protein (S1) binds to the host cell receptor Angiotensin converting enzyme 2 (ACE2). The region responsible for spike protein binding to ACE2 is the Receptor Binding Domain (RBD). The binding destabilizes the prefusion trimer, resulting in a post-fusion conformation. To engage the host the viral receptor undergoes hinge-like conformational movements that transiently hide or expose regions used during receptor binding, these two states are referred to as the “down” and “up” conformation, where down corresponds to the receptor-inaccessible state and up corresponds to the receptor-accessible state [2]. The region used during receptor binding is found to be closer to the central cavity of the trimer, compared to the closely related beta-coronaviruses [2].

As the underlying mechanism of the SARS-CoV-2 infection, the interaction between RBD of the spike protein and the ACE2 receptor has automatically been targeted for therapeutic antibody development and other applications. A wide variety of neutralizing monoclonal antibodies have been generated from hybridoma [4–6] or immunized organisms using recombinant technologies [7,8] have shown promising effects in inhibitory studies and a few have already been approved for treatment by the FDA [9,10].

Detailed knowledge of the specific interactions of pairs of antibodies and antigens, the epitope and paratope, respectively, are important during selection of antibodies for further development of therapeutic or prognostic use [11]. Furthermore, precise knowledge strengthens the IP protection of a given mAb. For development of therapeutic mAbs detailed knowledge of the epitope is a prerequisite for conducting clinical trials [12] and to increase the comparability between animal and human studies, when surrogate mAbs are to be used due to lacking cross-reactivity between species, both for safety and for proof-of-concept. A wide arsenal of techniques for the characterization of protein-protein binding interfaces is available [13,14]. Often these technologies complement each other and are used in combination to ensure highly confident results. However, the majority of the methods require prior assumptions of the structure of the interaction and are very labor intensive, making the methods unsuitable for early-stage Ab screening and selection. The methods used today are X-ray crystallography, Cryo electron microscopy, mutational scanning, hydrogen/ deuterium exchange (HDX-MS) [14–17], chemical cross-linking (CX-MS) [18–22], and chemical foot-printing [23–27]. All the methods require several sample handlings steps, which might alter the native structure of the protein in question.

Currently, the gold standard for Ab epitope mapping is X-ray crystallography. This is cumbersome work, with a very limited throughput. Thus, novel and more efficient methods are being sought. One such approach is based on hydrogen/deuterium-exchange in combination with MS. This has to some degree reduced the time needed to map epitopes, however, the method is relatively complicated and requires detailed data analysis. From the introduction of Fast Photochemical Oxidation of Proteins (FPOP) from Michael Gross’ laboratory [25,28], the Hydroxyl Radical Protein Footprinting (HRPF) has been utilized in epitope mapping. After

introduction into the field, several other alternatives have been implemented and especially with FOX systems [29], PLIMB [30], and X-ray activated hydroxyl radicals [27] showing promising results. However, the main problem with these systems is the need for specialized equipment, which is expensive to acquire and maintain. Fenton chemistry [31,32] that was first introduced in 1876 and 1934, use the reaction of Fe2+ with H_2O_2 to generate hydroxyl radicals. The hydroxyl radicals are one of the most powerful, nonselective, irreversible, and fast reacting radicals, which interact with both organic and inorganic compounds. The main reason that the field has not yet implemented the method is the slow reaction time of seconds to minutes, which can cause the protein to unfold or degrade upon oxidation. Compared to FPOP, that method has a reaction time in the millisecond time scale.

The use of controls within HRPF is essential to distinguish background from introduced oxidation, which is achieved by utilizing a sample that has not been subjected to oxidations [28,33]. Incorporation of biological replicates ensures that small variations do not create false positive results. Technical replicates should be utilized to minimize the variations between biological replicates. However, technical replicates are not generally reported [23,29,30,34,35] for this methodology. Furthermore, the analysis of antibody binding epitope by HRPF does not generally include non-binding antibodies (negative antibodies). The negative antibody control could be useful in removing false positive results (binding regions/paratope) when the interaction between the nonsense antibody and screened antigen occurs. The use of negative antibodies is very common in regular antibody experimental methodologies, as unspecific binding of nonsense antibodies is generally observed [36,37].

Commercially available instrumentation for epitope mapping is currently available but is not commonly used due to the high costs. In order to get the epitope mapping into the general mass spectrometric laboratory the overall costs must be decreased, or the methods coupled to existing infrastructure. This could be pipetting robots which in addition to higher throughput, increase reliability and reproducibility. Within this work, we have combined two different methods with different analysis methodologies, using surface plasmon resonance (SPR) and HRPF. From SPR two antibodies were selected to verify the binding and non-binding antibody, thereby allowing for the use of a true negative antibody control. HRPF was used as a method based on Fenton chemistry integrated into a semi-automized workflow on a pipetting robot. The combination of SPR and a semi-automated MS workflow allows to utilize the speed of SPR and the precision of HRPF. Biological triplicate analysis was performed for both the negative antibody control and the binding antibody. Furthermore, all samples were run in technical sextuplicate, to elucidate the technical variance. Stable isotope labeling in the form of TMT labelling was used as a quantification method, which is in contrast to the generally used label-free quantification [23,28,38].

The focus of the present investigation was epitope mapping of a mouse monoclonal antibody to the receptor binding domain of two SARS-CoV-2 spike protein variants (Wild-Type and variant B.1.617.2). The experimental setup utilizing multiple controls allowed for validation of false positive binding on several levels, while still being easily implementable in the general MS laboratory. The primary equipment needed to implement this method in addition to a mass spectrometer is a pipetting robot e.g., Opentrons OT-2.

Material and methods

Antigen production

The gene synthesized for expression of SARS-CoV-2 Spike RBD 319-541 WT (Wild-Type) variant has been based on the sequence GISAID: EPI_ISL_402119 (Denounced "Alpha" in this article). Variant B.1.617.2 (denounced commonly and further in this article as ''Delta'') has been based on the sequence EPI_ISL_2029113. Both constructs were synthesized commercially and cloned into pcDNA3.4-TOPO plasmid (Life Technologies B.V. Europe) that included a Tyr-Pho signal peptide and an N-terminal hexahistidine (6xHIS) tag. For both variants the expression was carried out in 25 mL culture using the Expi293F expression system (#A14635; ThermoFisher Scientific) according to manufacturer's instructions. Proteins harvested after 6 days post transfection were purified from the supernatant on a Ni-NTA Superflow column (#30430, Qiagen). Immediately after the elution protein fractions were buffer exchanged into PBS pH 7.4 using a HiPrep 26/10 Desalting column (#GE17-5087-01, Cytiva) and stored at -20°C. The purity and size of the protein has been evaluated by Sodium Dodecyl Sulfate Polyacrylamide gel electrophoresis (SDS-PAGE) using RunBlue (#ab270467 Abcam) 4-12% Bis-Tris polyacrylamide gel. Electrophoretic separation has been performed using Easy Power 500 (Invitrogen) in a non-reduced environment for 45 minutes at 200V at 110mA. The gel was stained with Coomassie Simply Blue Safe Stain (#LC6060 Invitrogen) and developed according to the manufacturer's instructions. Both SARS-CoV-2 Spike RBD 319-541 variants WT (#OBA0101, Ovodan Biotech) and variant B.1.617.2 (#OBA0105, Ovodan Biotech) have been donated by Ovodan Biotech A/S, Denmark (data sheets available in supplementary data).

Antibody

Monoclonal antibodies (mAbs) specific for receptor binding domain of two SARS-CoV-2 were generated by immunizing NMRI mice with recombinant RBD of SARS-CoV-2 (RBD, His Tag) (Sinobiological, number 40592-V08B). The mice were immunized twice subcutaneously, at an interval of 14 days, with 20 μg of the mixed with GERBU adjuvants (GERBU Biotechnik GmbH, Heidelberg, Germany). Fourteen days after the last injection and three days prior to fusion, the mice were immunized intravenously with recombinant RBD, and spleen cells were harvested and fused with myeloma cells, following the principles of Köhler and Milstein [39]. Supernatants from hybridomas were initially screened using Maxisorb ELISA plates (ThermoFisher Scientific, Roskilde, Denmark) coated with 0.5 µg/mL purified recombinant RBD followed by at least three rounds of cloning by limited dilution, ensuring clonality of the final hybridoma. Single clones were then grown in culture flasks in RPMI-1640 (Lonza, BioWhittaker, Basel, Switzerland) supplemented with sodium pyruvate (Gibco™, Waltham, MA, United States) and gentamicin sulfate (Biowest, Nuaillé, France) containing 10% fetal bovine serum (Biowest). Previously, developed and characterized antibody against peptidylarginine deiminase 4 (PAD4) was used as negative control.

Surface plasmon resonance analysis

Surface plasmon resonance (SPR) analysis was performed on a Biacore T200 instrument (Cytiva) and analyzed using Biacore T200 Evaluation Software (Cytiva). RBD variants were immobilized on a CM5 sensor chip using EDC/NHS chemistry at 10 µg/ml in a 10 mM acetic acid pH 5 buffer according to manufacturer's instructions.

Binding studies were performed at 10 µl/minute flow in the following running buffer: 140 mM NaCl, 10 mM Hepes, 0.1 Tween 20 pH 7.4 and the flow cells were regenerated with two injections of 20 µl a 100 mM H_3PO_4 between runs. All experiments were performed at least as triplicates of technical duplicates.

Samples

Biological triplicate samples were all prepared in a 96-well plate plate (Axygen, Corning incorporated), where they are lyophilized. Two experimental setups are run right after the other, the Control experiment (containing RBD Alpha and non-binding anti-PAD4 antibodies) and the Sample experiment (containing RBD Alpha and anti-RBD 20-14-5). Three sample types are prepared for both experiments: antibody, RBD Alpha or Delta, and a 1 to 1.5 molar ratio RBD and antibody. Each starting well contained 15 µg of protein.

Oxidative labelling

The oxidative labelling was performed on the Opentrons OT2 pipetting robot Opentrons Labworks, Inc., where the thermocycler module is used for cold cooling the sample. The robot was partially sealed and pressurized with nitrogen gas to decrease the oxygen level within the robot.

The samples were incubated in 32 µl footprinting buffer (FB) (10mM MOPSA/NaOH, 200mM NaCl, 10mM MgCl2) for 15 min. at 25°C, followed by aliquoting of the negative control (0 min incubation) sample into a new 96-well plate located in the thermocycler at 4°C. Each utilized well in the 96 well plate contained quenching buffer (QB) (0.1 M L-methionine) (10 µl for time zero and 20 µl for 3 and 9 min). Oxidative labelling was then prepared by addition of 6 µl Iron-EDTA (20 mM EDTA, 20 mM ammonium iron (II) sulfate hexahydride, in FB) (buffer mixed 30 min before use) and 6 µl 0.2 M Sodium ascorbate. The labelling was then initiated by the addition of 6 µl 10 mM freshly made hydrogen peroxide. All buffers were degassed prior to use, except for QB. Half the volume of each sample was transferred after 3 min of incubation to the microtiter plate in the thermocycler into 20 µl QB. The remainder of the samples were transferred after 9 min of incubation time to the thermocycler. To the 0 min incubation time sample 20 µl of 100 mM HEPES was added.

Sample preparation

The oxidative labelled samples were removed from the robot and the rest of the preparations were performed by hand. The samples were reduced by the addition of dithiothreitol (DTT) to a final concentration of 20 mM and incubated for 30 min at 57°C. This was followed by alkylation of the cysteines by the addition of Iodoacetamide (IAA) to a final concentration of 54 mM and incubated at RT in the dark for 20 min. The alkylation was stopped by the addition of 1 µl 0.1 M DTT.

The digestion was performed in three steps. 2 µl PNGaseF (P0705L, Glycerol-free, New England Biolabs) was added and incubated for one hour at 57°C. 2% LysC w/w (125-05061, Lysyl Endopeptidase Mass Spectrometry Grade, Fujifilm Wako Chemicals) was added and the incubation continued for an hour at 37°C and finally 2% methylated trypsin (methylated in-house) [40] was added and incubated for 10 hours at 37°C.

Samples were labelled by Tandem Mass Tag (TMT) 11plex according to the manufacturer's instructions, where 10 tags were used, and one common channel was used containing 1.5 µg of each sample from both experiments. All 10 tags were mixed in equal ratios for each biological replicate. The resulting 6 tubes containing 3 biological replicates for the Control and Sample experiment were micro-purified in accordance

with Rappsilber et al.[41], followed by lyophilization. For each biological replicate 6 purifications were performed resulting in a total of 36 lyophilized samples.

Mass spectrometry

Each sample was resuspended in 5.5 µl 0.1% FA before mass spectrometric analysis and transferred to a 96 well microtiter plate and loaded into an EASY-nLC™ 1200 system (Thermo Fisher Scientific). The LC system was connected to an Exploris 480 Orbitrap mass spectrometer (Thermo Fisher Scientific). Each biological replicate was run in six technical replicates using a 60 min gradient and the following main MS setting: Full scan: Orbitrap resolution of 120'000, scan range (m/z) of 350-1500, normalized AGC Target (%) of 300, maximum Injection Time Mode was set to Auto. Filters applied were MIPS: Monoisotopic peak determination of Peptide and Relax restrictions was set to True; Intensity: Filter type was Intensity Threshold set to 5.0e3; Data Dependent: Mode was Number of Scans with number of scans set to 10. Scan Event Type 1; Charged states used was 2-7 and undetermined charge states were not included; Dynamic exclusion: Exclude after 1 time, excluded for 60 seconds, mass tolerance was ±10ppm, Isotopes were excluded. Data dependent MS2 settings used were isolation window 0.8 m/z, HCD collision energy of 30%, Orbitrap resolution of 45000, First Mass of 110 m/z, Standard AGC Target, Maximum Injection Time Mode was Auto, Data type was Centroid.

The samples were run with a BSA standard for every third sample and three BSA standards between every biological replicate. The samples were run as follows: Sample experiment biological replicate 1 (SBRep1), Control experiment biological replicate 1 (CBRep1), SBRep2, CBRep2, SBRep3, and CBRep3.

Data analysis

The resulting 36 raw files from each experiment, 36 from RBD Alpha and 36 from RBD Delta, were searched in Proteome Discoverer 2.5 (Thermo Scientific). The files were recalibrated by quick search followed by several filtering steps. The spectra were filtered by signal to noise level of 1.5 and 10 peaks pr. 100 Da. Three rounds of searches were performed, the two first by the MASCOT search engine and the last with Sequest HT. Identified PSMs with a medium confidence or lower, where searched again for each round. The main search settings were 10 ppm precursor mass tolerance, 0.1 Da fragment mass tolerance, and two missed cleavages allowed. The following modifications were used for the MASCOT searches, for the first: Deamidation (NQ), Oxidation (P, F, D, M) Di-oxidation (M, W), and Carbonyl (S, V); and for the second: Deamidation (NQ), Oxidation (P, H, W, M, R, S), and Carbonyl (S, L, I). The last search by Sequest HT used the following modifications: Deamidation (NQ), Oxidation (D, F, H, K, M, N, P, Q, R, S, T, W, Y), Trioxidation (F, W, Y), and Carbonyl (A, E, I, L, P, Q, R, S, V). Ratios were calculated between all the conditions and the common channel, which were used for analysis. The resulting ratios for peptides groups were exported as CSV files including the following data, sequence, modifications in all possible sites, ratios, etc. (Example of full list can be seen in Supplementary data). Furthermore, the full modification list was exported for RBD Alpha or Delta depending on the experiment.

The data was imported into R studio [version, supplier] using an R markdown script, where the data was filtered and analyzed. Peptide groups were accepted if they were found in at least two out of three biological replicates and found in a single technical replicate pr. biological. Calculations of p-values using a two-sided Student's t-test were utilized. Ratios were average across the three biological replicates both for original data and for 3/0 min incubation and 9/0 min incubation, these were used for part of the analysis.

Ratio changes between antigen and antigen:antibody (Mix) were calculated by dividing the normalized abundance for 3 min or 9 min incubation with abundance for 0 min incubation within each sample type (Ag, Ab, or Mix). The values were then divided again between Mix and Ag or Mix and Ab, followed by averaging across the three biological replicates. For non-oxidized peptides values above 1 in the ratio between Mix and Ag or Mix and Ab indicate binding or shielding of the region, whereas values below 1 indicate an opening of the region. For oxidized peptides values below 1 in the ratio between Mix and Ag or Mix and Ab indicate binding or shielding of the region, whereas values above 1 indicate an opening of the region [42].

The mass spectrometry proteomics data have been deposited to the ProteomeXchange Consortium via the PRIDE [43] partner repository with the dataset identifier PXD046423.

Results

Antigen production

Two variants of the receptor binding domain of SARS-CoV-2 spike protein were expressed and purified. The alpha variant (RBD Alpha) and the delta variant (RBD Delta) were expressed and screened for correct location of mutations by mass spectrometry, where 93% coverage was achieved without PNGaseF and 100% coverage with PNGaseF for WT. That showed the presence of glycosylation on either or both potential sites. Expressed proteins were additionally tested by ELISA using anti-SARS-CoV-2 polyclonal IgY (OBP1121, Ovodan Biotech) confirming the presence of the protein. The size of the expressed RBD variant proteins has been determined by SDS-PAGE showing the expected size of 37 KDa for double glycosylated RBD aa 319-541. (Supplementary Figure 1).

Binding characterization

To characterize the binding between either RBDs to the anti-RBD antibody (20-14-5) and demonstrate the lack of binding to the negative control antibody (PAD4 14-11-3), binding kinetics were performed by SPR on both antigens and antibodies. The mAb 20-14-5 exhibited binding to both RBD Alpha and Delta in the nM range, with comparable affinities and kinetics, see Figure 1B. No binding to the control mAb (PAD4 14-11-3) was observed, see Figure 1A.

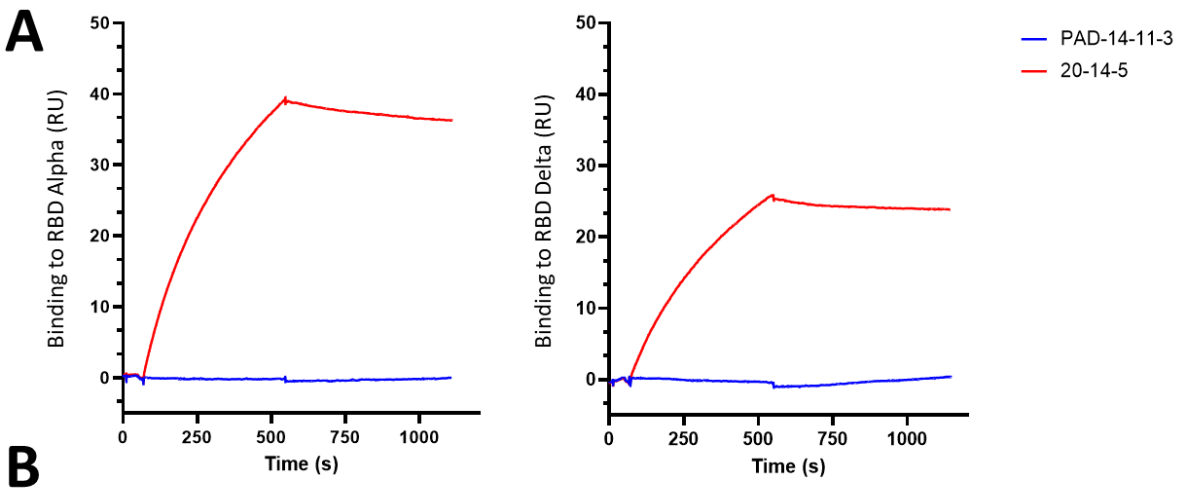

	k_a (10^4/Ms)	k_d (10^{-5}/s)	K_D (nM)
Alpha	5.8 ± 0.5	12.1 ± 1.3	2.1 ± 0.2
Delta	4.9 ± 0.7	8.2 ± 1.2	1.7 ± 0.5

Figure 1. A) SPR analysis of binding of 5 µ/ml 20-14-5 and control mAb (PAD-14-11-3) to RBD Alpha and Delta immobilized at densities of 0.036 and 0.041 pmol/mm2, respectively. B) Binding parameters for the binding of 20-14-5 to RBD Alpha and Delta, using 20-14-5.

Epitope mapping

The data generated from oxidative labelling was processed and tested for reproducibility with regard to biological and technical replicates. Technical replicates were evaluated in Figure 2A and E for RBD Alpha and Delta, respectively. For RBD Alpha the identification across all types of peptide groups shows an increasing trend for each additional technical replicate, where replicate 2 contributes an increase of 19.5%, and the following 13.9%, 10%, 8.2%, and 3.6% respectively. For RBD Delta the increase in identification from the technical replicate were 25%, 8.7%, 5.3%, 3%, and 7.8% respectively. The largest increase was observed for the first and second replicates for both RBD Alpha and Delta, whereas less increase was observed for the last three replicates. The full overview of increases by subcategory are presented in Supplementary Figure 3. A continual increase was expected, however less increase by additional replicates indicates that the depth of analysis is high and that additional replicates result in more identifications.

The modification patterns of RBD Alpha and Delta are shown in Figure 2B and F. Similar patterns were observed, with a high distribution of single oxidations, TMT labelling, and carbonylation. Difference in the tri-oxidation pattern is observed for the last part of the proteins, however, no modifications were observed for RBD Delta from 140 to 190. The TMT labelling was well distributed across the whole protein as expected for satisfactory labeling; however, a few missing areas are observed. The relatively low TMT labelling efficiency of 43% for RBD Alpha and 41% for RBD Delta may have caused the missing areas of labeling. However, this does not affect the conclusions drawn in this paper. The distribution of modified residues for each modification is shown in Supplementary Figure 2. Biological replicates showed a high identification rate of more than 65% in two out of three biological replicates across all samples. The overlap between biological

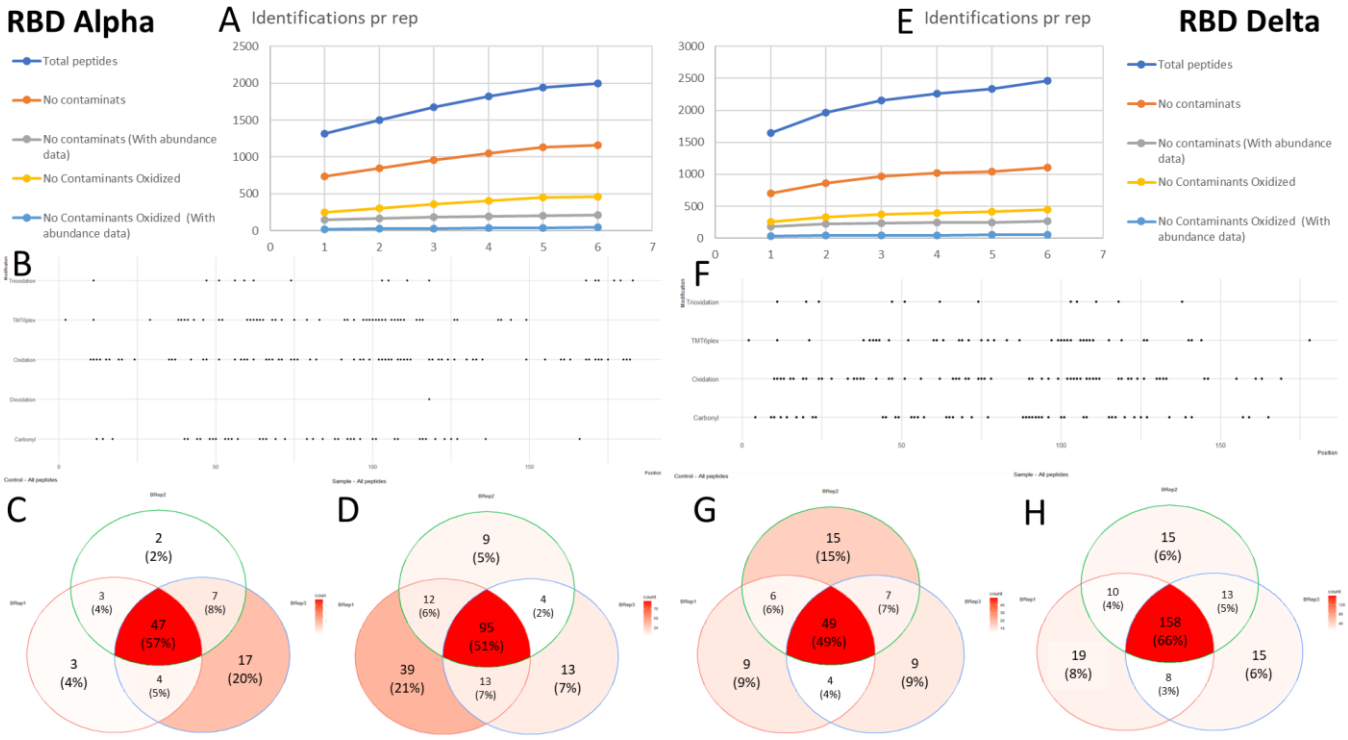

Figure 2. A and E show identified peptide groups depending on the number of technical replicates tested for RBD Alpha and Delta, respectively. Total peptide groups identified (Total peptides), no contaminants (Total, without contaminants), no contaminants with abundance data, no contaminants with oxidations, and no contaminants and oxidized with abundance data. B and F show the distribution of the modifications identified on RBD Alpha (B) and RBD Delta (F), modifications shown are Trioxidation, TMT-labeling, Oxidation, Dioxidation, and Carbonylation. C, D, G, and H show Venn Diagrams of biological replicates, for RBD Alpha (C and D) and RBD Delta (G and H), showing their overlap for Control and Sample experiments (a bit more explanation).

replicates was; for RBD Alpha 70% of control and 67% of sample and for RBD Delta 66% of control and 78% of sample (Figure 2C, D, G, and H).

Significant changes

Peptide groups extracted from Proteome Discoverer, with and without oxidative modifications, were analyzed for significant changes between the Ag and Ag + Ab (Mix) samples. All peptide groups identified with significant changes are presented in

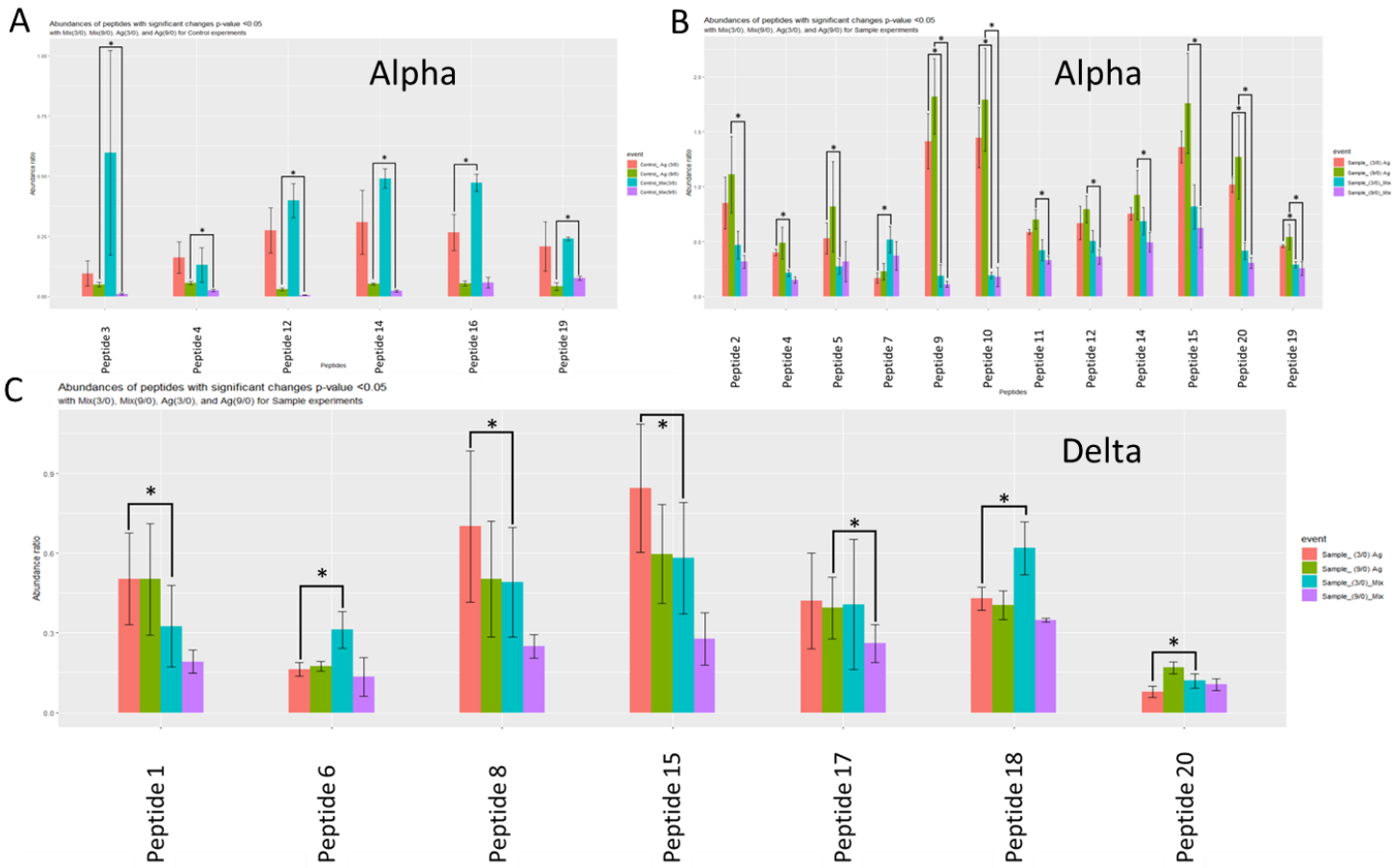

Figure 3. Peptides identified with at least one p-value of less than 0.05 at one time point. The colors represent different time point and sample type: Red = 3/0 min incubation for Ag, Green = 9/0 min incubation for Ag, Cyan = 3/0 min incubation for Mix, Purple = 9/0 min incubation for Mix. A) RBD Alpha Control experiment utilizing negative binding antibodies. B) RBD Alpha Sample experiment utilizing anti-RBD antibodies. C) RBD Delta Sample experiment utilizing anti-RBD antibodies.

Table 1. Each peptide group is renamed as peptide and numbered; the complete list is presented in Supplementary Figure 4. The resulting ratios elucidate the changes caused by mixing the two types of antibodies with the antigen. The significance of the changes was tested for each time point (3/0 min and 9/0 min incubation) and the significant peptide ratios are presented in Figure 3. Observed changes are translated into data that either represent a binding or an opening. Binding is achieved by lower abundance in the Ag sample for non-oxidized peptide groups and higher abundance in the Ag sample for oxidized peptide groups compared to the Mix sample. The binding can also be the result of shielding, which cannot be distinguished in this analysis. Binding can be observed between Ag and Ab samples whereas shielding is structural changes within the protein. However, an opening is a region with an increased exposure to the environment e.g., upon binding. An opening is achieved by higher abundance in the Ag sample for non-oxidized peptide groups and lower abundance in the Ag sample for oxidized peptide groups compared to the Mix sample.

Significant changes were observed for 6 peptides for RBD Alpha Control, with 3 peptides observed at 3/0 min and 3 peptides at 9/0 min incubation. Observed significant peptides span residues 357 to 514 on the intact spike protein. For RBD Alpha Sample, 12 peptides were identified spanning residues 356 to 534. Three peptides were found significantly changed at 3/0 min incubation and 5 peptides were found significantly changed at 9/0 min incubation. The remaining 4 peptides were found at both 3/0 min and 9/0 min incubation. A single peptide (Peptide 15) was identified with double oxidation and was identified at 9/0 min incubation. For RBD Delta, 6 peptides were observed with significant changes at 3/0 min incubation and 1 peptide at 9/0 min incubation, with peptides spanning from residue 328 to 534. Unlike the RBD Alpha Control, the RBD Delta Control did not show any significantly changed peptides.

The data from both RBD Alpha and Delta were combined to establish a common binding site, as we assume that the binding site is the same for both variants. Furthermore, a peptide has been categorized as a false positive if found in the Control experiment for RBD Alpha. Only the RBD Alpha Control experiment has been taken into consideration as no significant peptides were identified for RBD Delta Control. The non-binding negative control antibody, used in the control experiments, was confirmed to be non-binding by SPR shown in Figure 1. An overview of the peptides identified can be seen in Table 1. Calculations for binding or openings can be seen in Supplementary Figure 4. The resulting peptides identified with significant changes are peptide 1, 7, 9, 10, and 18 at 3/0 min incubation and peptide 2, 8, 9, 10, 15, 19, and 20 at 9/0 min incubation. Peptides that are found to have opposite data (binding or opening) have been marked with a question mark and are left out of the following analysis. Peptide 7 was identified to be involved in binding but is overlapping with three peptides showing an opening spanning residues 378 to 402. However, the data presented here shows only overlapping binding and opening and are therefore only conclusive for residues 392 to 395.

Table 1. Peptide groups identified for RBD Alpha and Delta Data are concatenated into either showing binding (B) or an opening (O). The data shown is from calculating Mix / Ag at 3/0- and 9/0-min incubation.

Peptide #	1. residue #	Last residue #	Molecular weight	Modifications	RBD Alpha				RBD Delta				RBD	
					Control		Sample		Control		Sample		Combined	
					3/0	9/0	3/0	9/0	3/0	9/0	3/0	9/0	3/0	9/0
Peptide 1	328	345	2328								O		O	
Peptide 2	356	378	2758					O						O
Peptide 3	357	368	1632			O							-	
Peptide 4	357	377	2602			O	O						-	
Peptide 5	357	385	3495				O						?	
Peptide 6	378	385	1140								B		?	
Peptide 7	392	402	1513				B						Bc	
Peptide 8	396	401	1036									O		O
Peptide 9	396	407	1592				O	O					O	O
Peptide 10	400	407	1172				O	O					O	O
Peptide 11	408	416	1128			O		O						-
Peptide 12	410	416	887			O		O						-
Peptide 13	424	443	1227								O		-	
Peptide 14	424	443	2495			O		O						-
Peptide 15	424	443	2527	2xOx				B						B
Peptide 16	424	443	2596		B								-	
Peptide 17	436	443	1120			O								-
Peptide 18	495	507	1656								B		B	
Peptide 19	508	514	1116		B		O	O					-	O
Peptide 20	508	534	3362				O	O			B		?	O

Binding site

Changes found to be significant were mapped to the three-dimensional structure of spike protein using the pdb structure 7mzg [44], shown in Figure 4. The peptides identified as significantly changed are mapped to the three-dimensional structure for RBD Alpha Control experiment, shown in Figure 4A. Binding is observed at 3/0 min of incubation for two parallel beta sheets, peptide 16 and peptide 19, with unstructured regions in each end. However, several regions show opening for 9/0 min of incubation, including one of the same regions that showed binding but with another peptide, peptide 14. The other regions identified with an opening are peptide 3, 4, 11, 12, and 17. None of the identified peptides were found as significant at both time points.

For the RBD Alpha Sample experiment, Figure 4B, the regions of residue 396 to 407 and 508 to 534 (peptides 9 and 10) were found to show opening upon binding to the antibody for both time points, 3/0 min and 9/0 min incubation. Openings were also observed for region 357 to 385 at 3/0 min incubation (peptide 4 and 5), whereas, for 9/0 min incubation openings were observed for regions 356 to 378, 400 to 416, and 424 to 443 (peptide 2, 11, 12, and 14). Binding was observed for the Alpha Sample experiment at region 392 to 402 for 3/0 min incubation (peptide 7), and 424 to 443 for 9/0 min incubation when a double oxidation is present (peptide 15).

For the RBD Delta Sample experiment, Figure 4C, openings were observed for regions 328 to 345 and 424 to 443 for 3/0 min incubation (peptide 1 and 13). Binding at 3/0 min incubation were observed for region 378 to 385 and 495 to 534 (peptide 6, 18, and 20). For 9/0 min incubation, only region 436 to 443 was observed with an opening (peptide 8).

The significant changes observed for RBD Alpha and Delta were combined as described previously and mapped to the three-dimensional structure shown in Figure 4D. This data shows two primary binding sites, one in the top of the RBD, generally accessible, and the second located on the inside towards the center of the trimer. To simplify the binding site, only the regions showing binding, were mapped to the structure and the two time points were combined, shown in Figure 4E. Binding of anti-RBD to RBD Alpha and Delta was mapped to region 495 to 507 and the double oxidized region 424 to 443, peptide 18 and 15, respectively. The binding was additionally mapped to the trimer of spike protein, where it was mapped to the open conformation of spike protein, Figure 4F.

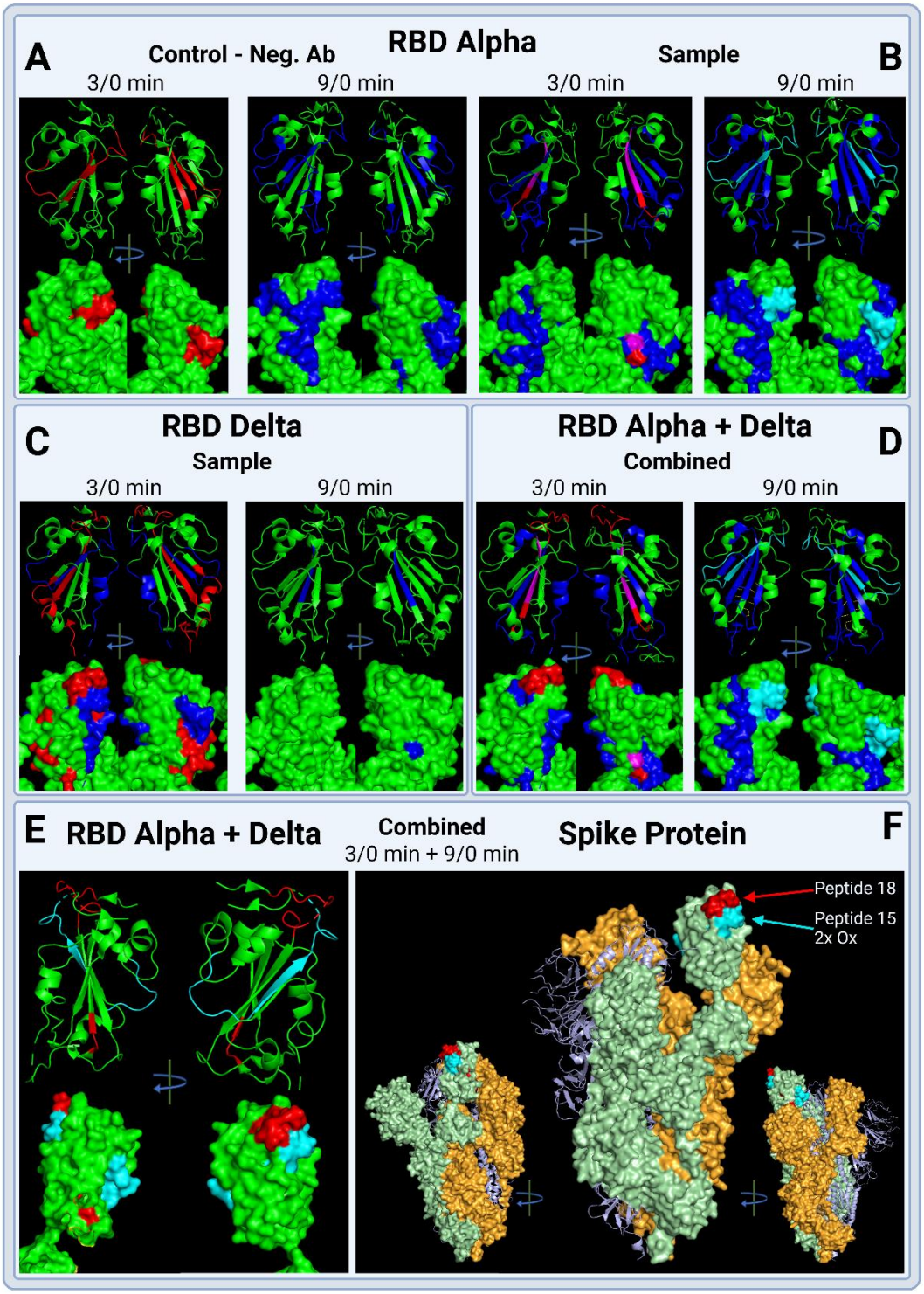

Figure 4. Three-dimensional structure of Receptor Binding Domain (RDB) from SARS-CoV2 spike protein. The pdb structure pdb7mzg was utilized to map the significant changes. The changes are colored the following: Red = Binding/shielding (Decreased exposure), Blue = Opening (Increased exposure), Magenta = found to be both binding and opening, Cyan = Binding of double oxidized peptide. A) RBD Alpha Control experiment with negative antibodies for 3/0 min and 9/0 min incubation. B) RBD Alpha Sample experiment with anti-RBD antibodies for 3/0 min and 9/0 min incubation. C) RBD Delta Sample experiment with anti-RBD antibodies. C) Combined data for RBD Alpha and RBD Delta Sample experiment with anti-RBD antibodies for 3/0 min and 9/0 min incubation. Data from the Control experiment have been subtracted from the combined data. E) Combined data for RBD Alpha and RBD Delta Sample experiment with anti-RBD antibodies for 3/0 min and 9/0 min incubation. Only the binding data are shown. F) Combined data for RBD Alpha and RBD Delta Sample experiment with anti-RBD antibodies for 3/0 min and 9/0 min incubation. Mapped to the complete spike protein. Each protein was distinguished by color; green, orange, and light purple, respectively.

Discussion

The currently used methods within HRPF analysis of protein-protein interactions have a number of shortcomings. The problems in particular, are linked to a wide variety of modification outcomes, low dynamic range, and reliability of the quantification used. We therefore set out to make an experimental setup of paratope-epitope mapping with hydroxyl radical protein footprinting (HRPF) using Fenton chemistry, that could be reliable while still using relative long incubation times (3 min and 9 min). The following controls were introduced to increase the reliability and robustness of the data: no oxidation controls (0 min incubation) for all samples, six times technical replicates, biological triplicates, and a negative control antibody that does not bind the antigen. Unlike the majority of current HRPF experimental setups [23–27] we introduced a stable isotope labelling strategy by incorporating TMT labelling for relative quantification.

Quantification of HRPF data is problematic due to the known introduction of a large number of PTMs across the entire protein, thereby increasing the complexity of the sample. Furthermore, the stoichiometry of the introduced oxidation and other PTMs are low, which is problematic when using data dependent acquisition (DDA) methods. The current DDA method incorporated a long exclusion time in addition to 6 technical replicates for all samples in order to increase the depth of the analysis. Compared to the literature, most studies using FPOP focus on a single non-oxidation control and biological triplicates [35,45]. Alternatively biological duplicates for both oxidized and non-oxidized control have been used [23,46]. New technologies have recently been introduced, employing HRPF for epitope mapping. These methods have generally used 3 biological replicates for both oxidized and non-oxidized samples [29,30]. Common to all of the above-mentioned works is the analysis of two proteins and their binding epitope, where each protein is analysed alone and in combination. However, none of these studies included negative non-binding control antibodies (neg. Ab) or decoy proteins. The use of these neg. Ab or decoy proteins could prove essential in minimalizing the false discovery rate. We have shown in Figure 4A that significant changes can be recorded even though no binding was observed by SPR, Figure 1. The use of neg. Ab is common practice within the antibody research field, as antibodies are notorious for having unspecific binding. We therefore encourage others to utilize this in their work, as it proved to exclude several peptides from the final analysis e.g., peptide 3, 4, 11, 12, 13, 14, 16, and 17. This, reduced the significantly changed peptides from 20 to 12, corresponding to a false positive rate of 40% of the identified peptides with significant changes.

The TMT labelling strategy allowed us to decrease the number of samples to be processed and at the same time limit the number of missing values across samples. Furthermore, by the use of the TMT common channel we were able to normalize all samples and directly compare ratios across sample types and between control and sample experiments. The relative quantification showed that both increases and decreases in abundance could be analysed for both non-oxidized and oxidized peptides, corresponding to binding and openings of regions.

The present epitope mapping approach is based on Fenton chemistry and is not to the authors knowledge commercially available through contract research organizations. Other methodologies using hydroxyl radical protein footprinting (HRPF) are both available within academia and commercially. Fast Photochemical Oxidation of Proteins (FPOP), invented by Gross' laboratory [25,28], promised wide use but due to high cost of implementation and safety hazards of the laser, the method has not been put into practice in the standard laboratory[29]. Therefore, several other applications for HRPF have been suggested with X-ray activated HRPF by Jain et al.[27], Flash Oxidation system (FOX) by Sharp et al.[29], and Plasma-Induced Modification of Biomolecules (PLIMB) by Sussman et al.[30]. All the methods mentioned above have the same shortcoming

regarding implementation; a specific instrument is needed to perform the chemistry prior to sample preparation and analysis by mass spectrometry. For the development of our approach, we set out to make the experimental setup more robust and integrate standards from both antibody research and proteomics with regards to negative control antibodies, biological and technical replicates.

The main drawback of Fenton chemistry, which has been addressed several times in the available literature regarding HRPF, is the time scale of the reaction, ranging from several seconds to minutes [29]. This time scale does not allow for investigation of protein dynamics but could prove useful when identifying antibody-antigen interactions due to the high stability. The introduction of controls on several levels combined with semi-automatic sample handling by pipetting robot, achieves high level of reproducibility and robustness. The method shown in the present work should be widely applicable and easily implementable as the only additional equipment needed is a pipetting robot. Such equipment has recently become more common due to increased sample load combined with faster mass spectrometers.

The binding epitope identified by our experimental setup found that anti-RBD bound to both RBD Alpha and Delta at residues 392 to 402, 424 to 443 when double oxidized, and 495 to 507, peptide 7, 15, and 18 respectively. The region identified here as the binding epitope matches that found by both Yuan et al. [47] and Wu et al. [48]. The binding site mapped to the complete trimer of SARS-Cov-2 spike protein, shown in Figure 4F, showed that the binding site is located on the tip of the receptor binding domain and is accessible in both closed and open structure [49].

Conclusion

The use of negative antibody controls within hydroxyl radical protein footprinting (HRPF) has not been widely applied. The use of negative antibody control is however, generally applied within antibody research. We demonstrated that 40% of the identified peptides with a significant change were false positives by using negative antibody controls. Direct comparison across sample types and conditions were applicable due to TMT labeling. Furthermore, the introduction of TMT labeling, semi-automatic sample handling, biological triplicates, and six technical replicates, achieved data with great depth of analysis and reliability.

The binding epitope that was identified on receptor binding domain from SARS-CoV-2 spike protein variant Alpha and Delta, were residue 392 to 402, 424 to 443 when double oxidized, and 495 to 507, peptide 7, 15, and 18 respectively. The identified binding site matches the one found in the previous epitope mapping studies of anti-RBD SARS-Cov-2 neutralizing antibodies.

This work should be of great use and inspiration to increase the reliability of mass spectrometric based epitope mapping methodologies. The inclusion of a few extra controls allows for increased depth of analysis and the ability to determine the false discovery rate by the method.

In conclusion we suggest that the combination of experimental controls and stable isotope labelling strategy should be implemented widely to ensure the limitation of false discovery in the HRPF epitope mapping. This will considerably minimize the risk of wrongly assigned peptides in binding sites for epitope mapping.

References

[1] Gorbalenya AE, Baker SC, Baric RS, de Groot RJ, Drosten C, Gulyaeva AA, et al. The species Severe acute respiratory syndrome-related coronavirus: classifying 2019-nCoV and naming it SARS-CoV-2. Nat Microbiol 2020;5:536–44. https://doi.org/10.1038/s41564-020-0695-z.

[2] Wrapp D, Wang N, Corbett KS, Goldsmith JA, Hsieh C-L, Abiona O, et al. Cryo-EM structure of the 2019-nCoV spike in the prefusion conformation. Science (80-) 2020;367:1260–3. https://doi.org/10.1126/science.abb2507.

[3] Monteil V, Kwon H, Prado P, Hagelkrüys A, Wimmer RA, Stahl M, et al. Inhibition of SARS-CoV-2 Infections in Engineered Human Tissues Using Clinical-Grade Soluble Human ACE2. Cell 2020;181:905-913.e7. https://doi.org/10.1016/j.cell.2020.04.004.

[4] Shi R, Shan C, Duan X, Chen Z, Liu P, Song J, et al. A human neutralizing antibody targets the receptor-binding site of SARS-CoV-2. Nature 2020;584:120–4. https://doi.org/10.1038/s41586-020-2381-y.

[5] Rappazzo CG, Tse L V., Kaku CI, Wrapp D, Sakharkar M, Huang D, et al. Broad and potent activity against SARS-like viruses by an engineered human monoclonal antibody. Science (80-) 2021;371:823–9. https://doi.org/10.1126/science.abf4830.

[6] Pinto D, Park Y-J, Beltramello M, Walls AC, Tortorici MA, Bianchi S, et al. Cross-neutralization of SARS-CoV-2 by a human monoclonal SARS-CoV antibody. Nature 2020;583:290–5. https://doi.org/10.1038/s41586-020-2349-y.

[7] Bertoglio F, Meier D, Langreder N, Steinke S, Rand U, Simonelli L, et al. SARS-CoV-2 neutralizing human recombinant antibodies selected from pre-pandemic healthy donors binding at RBD-ACE2 interface. Nat Commun 2021;12:1577. https://doi.org/10.1038/s41467-021-21609-2.

[8] Favorskaya IA, Shcheblyakov D V., Esmagambetov IB, Dolzhikova I V., Alekseeva IA, Korobkova AI, et al. Single-Domain Antibodies Efficiently Neutralize SARS-CoV-2 Variants of Concern. Front Immunol 2022;13. https://doi.org/10.3389/fimmu.2022.822159.

[9] Food and Drug Administration. Fact sheet for healthcare providers: Emergency Use Authorization for Evusheld (tixagevimab co-packaged with cilgavimab n.d. https://www.fda.gov/media/154701/download (accessed October 15, 2023).

[10] Food and Drug Administration. Fact sheet for healthcare providers: Emergency Use Authorization (EUA) of sotrovimab. FDA n.d. https://www.fda.gov/media/149534/download (accessed October 15, 2023).

[11] Petta I, Lievens S, Libert C, Tavernier J, De Bosscher K. Modulation of Protein–Protein Interactions for the Development of Novel Therapeutics. Mol Ther 2016;24:707–18. https://doi.org/10.1038/mt.2015.214.

[12] Ditto NT, Brooks BD. The emerging role of biosensor-based epitope binning and mapping in antibody-based drug discovery. Expert Opin Drug Discov 2016;11:925–37. https://doi.org/10.1080/17460441.2016.1229295.

[13] Hayes S, Malacrida B, Kiely M, Kiely PA. Studying protein–protein interactions: progress, pitfalls and

solutions. Biochem Soc Trans 2016;44:994–1004. https://doi.org/10.1042/BST20160092.

[14] Zhou M, Li Q, Wang R. Current Experimental Methods for Characterizing Protein–Protein Interactions. ChemMedChem 2016;11:738–56. https://doi.org/10.1002/cmdc.201500495.

[15] Zhang Z, Smith DL. Determination of amide hydrogen exchange by mass spectrometry: A new tool for protein structure elucidation. Protein Sci 1993;2:522–31. https://doi.org/10.1002/pro.5560020404.

[16] Katta V, Chait BT, Carr S. Conformational changes in proteins probed by hydrogen-exchange electrospray-ionization mass spectrometry. Rapid Commun Mass Spectrom 1991;5:214–7. https://doi.org/10.1002/rcm.1290050415.

[17] Johnson RS, Walsh KA. Mass spectrometric measurement of protein amide hydrogen exchange rates of apo- and holo-myoglobin. Protein Sci 1994;3:2411–8. https://doi.org/10.1002/pro.5560031224.

[18] Kostyukevich Y, Acter T, Zherebker A, Ahmed A, Kim S, Nikolaev E. Hydrogen/deuterium exchange in mass spectrometry. Mass Spectrom Rev 2018;37:811–53. https://doi.org/10.1002/mas.21565.

[19] O'Reilly FJ, Rappsilber J. Cross-linking mass spectrometry: methods and applications in structural, molecular and systems biology. Nat Struct Mol Biol 2018;25:1000–8. https://doi.org/10.1038/s41594-018-0147-0.

[20] Schneider M, Belsom A, Rappsilber J. Protein Tertiary Structure by Crosslinking/Mass Spectrometry. Trends Biochem Sci 2018;43:157–69. https://doi.org/10.1016/j.tibs.2017.12.006.

[21] Chen ZA, Rappsilber J. Protein structure dynamics by crosslinking mass spectrometry. Curr Opin Struct Biol 2023;80. https://doi.org/10.1016/j.sbi.2023.102599.

[22] Yu C, Huang L. Cross-Linking Mass Spectrometry: An Emerging Technology for Interactomics and Structural Biology. Anal Chem 2018;90:144–65. https://doi.org/10.1021/acs.analchem.7b04431.

[23] Loginov DS, Fiala J, Brechlin P, Kruppa G, Novak P. Hydroxyl radical footprinting analysis of a human haptoglobin-hemoglobin complex. Biochim Biophys Acta - Proteins Proteomics 2022;1870. https://doi.org/10.1016/j.bbapap.2021.140735.

[24] Gau, Brian and Garai, Kanchan and Frieden, Carl and Gross ML. Mass spectrometry-based protein footprinting characterizes the structures of oligomeric apolipoprotein E2, E3, and E4. Biochemistry 2011;50:8117–26.

[25] Li, Ke Sherry and Shi, Liuqing and Gross ML. Mass spectrometry-based fast photochemical oxidation of proteins (FPOP) for higher order structure characterization. Acc Chem Res 2011;51:736–44.

[26] Kiselar J, Chance MR. High-Resolution Hydroxyl Radical Protein Footprinting: Biophysics Tool for Drug Discovery 2018. https://doi.org/10.1146/annurev-biophys.

[27] Jain R, Dhillon NS, Farquhar ER, Wang B, Li X, Kiselar J, et al. Multiplex Chemical Labeling of Amino Acids for Protein Footprinting Structure Assessment. Anal Chem 2022;94:9819–25. https://doi.org/10.1021/acs.analchem.2c01640.

[28] Gau B, Garai K, Frieden C, Gross ML. Mass spectrometry-based protein footprinting characterizes the structures of oligomeric apolipoprotein E2, E3, and E4. Biochemistry 2011;50:8117–26.

https://doi.org/10.1021/bi200911c.

[29] Sharp JS, Chea EE, Misra SK, Orlando R, Popov M, Egan RW, et al. Flash Oxidation (FOX) System: A Novel Laser-Free Fast Photochemical Oxidation Protein Footprinting Platform. J Am Soc Mass Spectrom 2021;32:1601–9. https://doi.org/10.1021/jasms.0c00471.

[30] Minkoff BB, Blatz JM, Choudhury FA, Benjamin D, Shohet JL, Sussman MR. Plasma-Generated OH Radical Production for Analyzing Three-Dimensional Structure in Protein Therapeutics. Sci Rep 2017;7. https://doi.org/10.1038/s41598-017-13371-7.

[31] Fenton HJH. On a new reaction of tartaric acid. Chem News 1876;33:190.

[32] Koppenol WH. The Haber-Weiss cycle - 70 years later. Redox Rep 2001;6:229–34. https://doi.org/10.1179/135100001101536373.

[33] Ralston CY, Sharp JS. Structural Investigation of Therapeutic Antibodies Using Hydroxyl Radical Protein Footprinting Methods. Antibodies 2022;11. https://doi.org/10.3390/antib11040071.

[34] Lin M, Krawitz D, Callahan MD, Deperalta G, Wecksler AT. Characterization of ELISA Antibody-Antigen Interaction using Footprinting-Mass Spectrometry and Negative Staining Transmission Electron Microscopy. J Am Soc Mass Spectrom 2018;29:961–71. https://doi.org/10.1007/s13361-017-1883-9.

[35] Schick AJ, Lundin V, Low J, Peng K, Vandlen R, Wecksler AT. Epitope mapping of anti-drug antibodies to a clinical candidate bispecific antibody. MAbs 2022;14. https://doi.org/10.1080/19420862.2022.2028337.

[36] Shembekar N, Hu H, Eustace D, Merten CA. Single-Cell Droplet Microfluidic Screening for Antibodies Specifically Binding to Target Cells. Cell Rep 2018;22:2206–15. https://doi.org/10.1016/j.celrep.2018.01.071.

[37] Pochechueva T, Chinarev A, Bovin N, Fedier A, Jacob F, Heinzelmann-Schwarz V. PEGylation of microbead surfaces reduces unspecific antibody binding in glycan-based suspension array. J Immunol Methods 2014;412:42–52. https://doi.org/10.1016/j.jim.2014.06.015.

[38] Polák M, Yassaghi G, Kavan D, Filandr F, Fiala J, Kukačka Z, et al. Utilization of Fast Photochemical Oxidation of Proteins and Both Bottom-up and Top-down Mass Spectrometry for Structural Characterization of a Transcription Factor-dsDNA Complex. Anal Chem 2022;94:3203–10. https://doi.org/10.1021/acs.analchem.1c04746.

[39] COTTON RGH, MILSTEIN C. Fusion of Two Immunoglobulin-producing Myeloma Cells. Nature 1973;244:42–3. https://doi.org/10.1038/244042a0.

[40] Heissel S, Frederiksen SJ, Id JB, Peter H. Enhanced trypsin on a budget : Stabilization , purification and high-temperature application of inexpensive commercial trypsin for proteomics applications 2019:1–16.

[41] Rappsilber J, Mann M, Ishihama Y. Protocol for micro-purification, enrichment, pre-fractionation and storage of peptides for proteomics using StageTips. Nat Protoc 2007;2:1896.

[42] Leser M, Chapman JR, Khine M, Pegan J, Law M, Makkaoui M El, et al. Chemical Generation of Hydroxyl Radical for Oxidative 'Footprinting.' Protein Pept Lett 2019;26:61–9.

https://doi.org/10.2174/0929866526666181212164812.

[43] Perez-Riverol Y, Bai J, Bandla C, García-Seisdedos D, Hewapathirana S, Kamatchinathan S, et al. The PRIDE database resources in 2022: a hub for mass spectrometry-based proteomics evidences. Nucleic Acids Res 2022;50:D543–52. https://doi.org/10.1093/nar/gkab1038.

[44] Wheatley AK, Pymm P, Esterbauer R, Dietrich MH, Lee WS, Drew D, et al. Landscape of human antibody recognition of the SARS-CoV-2 receptor binding domain. Cell Rep 2021;37:109822. https://doi.org/10.1016/j.celrep.2021.109822.

[45] Lin M, Krawitz D, Callahan MD, Deperalta G, Wecksler AT. Characterization of ELISA Antibody-Antigen Interaction using Footprinting-Mass Spectrometry and Negative Staining Transmission Electron Microscopy. J Am Soc Mass Spectrom 2018;29:961–71. https://doi.org/10.1007/s13361-017-1883-9.

[46] Jiang R, Rempel DL, Gross ML. MALDI peptide mapping for fast analysis in protein footprinting. Int J Mass Spectrom 2023;490. https://doi.org/10.1016/j.ijms.2023.117080.

[47] Yuan M, Liu H, Wu NC, Lee C-CD, Zhu X, Zhao F, et al. Structural basis of a shared antibody response to SARS-CoV-2. Science (80-) 2020;369:1119–23. https://doi.org/10.1126/science.abd2321.

[48] Wu Y, Wang F, Shen C, Peng W, Li D, Zhao C, et al. A noncompeting pair of human neutralizing antibodies block COVID-19 virus binding to its receptor ACE2. Science (80-) 2020;368:1274–8. https://doi.org/10.1126/science.abc2241.

[49] Francino-Urdaniz IM, Whitehead TA. An overview of methods for the structural and functional mapping of epitopes recognized by anti-SARS-CoV-2 antibodies. RSC Chem Biol 2021;2:1580–9. https://doi.org/10.1039/d1cb00169h.

Receptor binding domain of SARS-CoV-2 Spike protein Wild Type (Wuhan)

The coverage obtained for **Tryp_CoV_2 was 92.74%.** Green have been observed, black not observed, highlighted is the possible glycosylation sites. Total peptide spectra = 166 and unique peptides spectra = 89.

HHHHHHHHHHFTVEKGIYQTSNFRVQPTESIVRFPNITNLCPFGEVFNATRFASVYAWNRKRIS
NCVADYSVLYNSASFSTFKCYGVSPTKLNDLCFTNVYADSFVIRGDEVRQIAPGQTGKIADYNYK
LPDDFTGCVIAWNSNNLDSKVGGNYNYLYRLFRKSNLKPFERDISTEIYQAGSTPCNGVEGFNC
YFPLQSYGFQPTNGVGYQPYRVVVLSFELLHAPATVCGPKKSTNLVKNKCVNFNF

The coverage obtained for **Tryp_PNGaseF_CoV_2 was 100%.** Green have been observed, black not observed, highlighted is the possible glycosylation sites. Red are deamidated aparagines indicating previous glycosylation Total peptide spectra = 196 and unique peptides spectra = 95.

HHHHHHHHHHFTVEKGIYQTSNFRVQPTESIVRFPNITNLCPFGEVFNATRFASVYAWNRKRIS
NCVADYSVLYNSASFSTFKCYGVSPTKLNDLCFTNVYADSFVIRGDEVRQIAPGQTGKIADYNYK
LPDDFTGCVIAWNSNNLDSKVGGNYNYLYRLFRKSNLKPFERDISTEIYQAGSTPCNGVEGFNC
YFPLQSYGFQPTNGVGYQPYRVVVLSFELLHAPATVCGPKKSTNLVKNKCVNFNF

Receptor binding domain of SARS-CoV-2 Spike protein Delta

Triplicate MS analysis were performed from the same digestion. From here a coverage of 84.62% was achieved. The coverage of the peptide FPNITNLCPFGEVFNATR was not possible to identify, which was expected due to known glycosylation on N(IT) and N(AT). Furthermore, the signal peptide was not identified as well, as expected.

```
MGILPSPGMP ALLSLVSLLS VLLMGCVAFR VQPTESIVRF PNITNLCPFG EVFNATRFAS   60
VYAWNRKRIS NCVADYSVLY NSASFSTFKC YGVSPTKLND LCFTNVYADS FVIRGDEVRQ  120
IAPGQTGKIA DYNYKLPDDF TGCVIAWNSN NLDSKVGGNY NYRYRLFRKS NLKPFERDIS  180
TEIKQAGSTP CNGVEGFNCY FPLQSYGFQP TNGVGYQPYR VVVLSFELLH APATVCGPKK  240
STNLVKNKCV NFGHHHHHHH      260
Coverage: 220/260  84.62%   sp|P0DTC2|SPIKE_SARS2_Delta2 RBD Spike glycoprotein OS=Severe acute r
```

These data are in accordance with the data obtained for the other RBD variants, where a deeper analysis was carried out.

Supplementary Figure 1. Sequence validation by mass spectrometry of RBD Alpha and Delta where two glycosylation sites have been identified.

Supplementary Figure 2. Identified modifications and their residue distribution for each RBD Wuhan (Blue) and RBD Delta (Red). Modifications shown are: Single oxidation, dioxidation, trioxidation, carbonylation, and TMT labeling.

RBD Delta											
#reps	Total peptides	No contaminats	No contaminats (With	No Contaminants Oxidized	No Contaminants Oxidized (With	Increases upon addition of more replicates					
1	1644	704	180	253	34	Total peptides	No contaminats	No contaminats (With	No Contaminan	No Contaminan	Avg
2	1961	865	221	329	44	1.193	1.229	1.228	1.300	1.294	1.249
3	2150	966	230	373	46	1.096	1.117	1.041	1.134	1.045	1.087
4	2257	1017	243	397	48	1.050	1.053	1.057	1.064	1.043	1.053
5	2334	1038	241	413	51	1.034	1.021	0.992	1.040	1.063	1.030
6	2467	1100	262	442	57	1.057	1.060	1.087	1.070	1.118	1.078

RBD Alpha											
#reps	Total peptides	No contaminats	No contaminats (With	No Contaminants Oxidized	No Contaminants Oxidized (With	Increases upon addition of more replicates					
1	1318	737	148	249	22	Total peptides	No contaminats	No contaminats (With	No Contaminan	No Contaminan	Avg
2	1499	846	167	304	29	1.137	1.148	1.128	1.221	1.318	1.191
3	1679	961	182	357	34	1.120	1.136	1.090	1.174	1.172	1.139
4	1820	1051	193	407	38	1.084	1.094	1.060	1.140	1.118	1.099
5	1942	1136	207	452	41	1.067	1.081	1.073	1.111	1.079	1.082
6	1999	1159	214	462	44	1.029	1.020	1.034	1.022	1.073	1.036

Supplementary Figure 3. Identified peptide groups in different subcategories for each additional technical replicate. Increases of each technical replicate can be seen in the last column below "Increases upon addition of more replicates".

Control RBD Wuhan	3 min			9 min			Type (Non-Ox) 3 min			Type (Non-Ox) 9 min			Type (Ox) 3 min			Type (Ox) 9 min		
	Mix	Ag	Mix/Ag	Mix	Ag	Mix/Ag	Binding	No change	Opening	Binding	No change	Opening	Binding	No change	Opening	Binding	No change	Opening
39 (2602) (39-59)	-	-	-	0.025	0.05	0.50						x						
39 (1632) (39-50)	-	-	-	0.01	0.05	0.20						x						
55 (1750) (55-67)	0.05	0.04	1.29	-	-	-	x											
106 (2596) (106-125)	0.47	0.27	1.76	-	-	-	x											
106 (2495) (106-125)	-	-	-	0.022	0.05	0.44						x						
177 (1656) (177-189)	0.47	0.10	4.70	-	-	-	x											

Sample RBD Wuhan	3 min			9 min			Type (Non-Ox)			Type (Non-Ox)			Type (Ox) 3 min			Type (Ox) 9 min		
	Mix	Ag	Mix/Ag	Mix	Ag	Mix/Ag	Binding	No change	Opening	Binding	No change	Opening	Binding	No change	Opening	Binding	No change	Opening
38 (2758) (38-60)	-	-	-	0.3	1.1	0.27						x						
39 (3494) (39-67)	0.27	0.53	0.51	-	-	-			x									
39 (2602) (39-60)	0.20	0.40	0.50	0.15	0.50	0.30			x			x						
74 (1513) (74-84	0.50	0.17	2.94	0.37	0.22	1.68	x			x								
78 (1592) (78-89)	0.17	1.35	0.13	0.11	1.48	0.07			x			x						
82 (1172) (82-89)	0.17	1.48	0.11	0.17	1.74	0.10			x			x						
90 (1128) (90-98)	-	-	-	0.33	0.70	0.47						x						
92 (887) (92-98)	-	-	-	0.36	0.80	0.45						x						
93 (816) (93-98)	-	-	-	0.167	0.81	0.21						x						
106 (2495) (106-125)	-	-	-	0.49	0.92	0.53						x						
106 (2527) (106-125) (Ox)	-	-	-	0.62	1.75	0.35										x		
106 (2528) (106-125) (Ox)	0.78	1.48	0.53	0.58	1.67	0.35							x			x		
177 (1657) (177-189)	0.87	0.10	8.72	0.65	0.18	3.71	x			x								
190 (3362) (190-216)	0.41	1.02	0.40	0.31	1.27	0.24			x			x						
190 (1115) (190-196)	0.25	0.46	0.54	0.23	0.53	0.43			x			x						

Sample - RBD Delta	3 min			9 min			Type (Non-Ox) 3 min			Type (Non-Ox) 9 min			Type (Ox) 3 min			Type (Ox) 9 min		
	Mix	Ag	Mix/Ag	Mix	Ag	Mix/Ag	Binding	No change	Opening	Binding	No change	Opening	Binding	No change	Opening	Binding	No change	Opening
10 (2328) (10-27)	0.32	0.5	0.64	-	-	-			x									
60 (1140) (60-67)	0.31	0.16	1.9375	-	-	-	x											
78 (1036) (78-83)	0.49	0.7	0.7	-	-	-			x									
106 (1227) (106-125)	0.58	0.84	0.690476	-	-	-			x									
118 (1120) (118-125)	-	-	-	0.26	0.39	0.666667						x						
177 (1656) (177-189)	0.62	0.43	1.44186	-	-	-	x											
190 (3362) (190-216)	0.12	0.079	1.518987	-	-	-	x											

Supplementary Figure 4. Table of identified peptides with a p-value of 0.05 or less and their corresponding ratio abundances. Mig/Ag abundances are calculated and type of binding/shielding, no change, or an opening is marked. Data for both Control and Sample experiments for RBD Wuhan is shown along with data from Sample experiment for RBD Delta, as no significant changes were observed for RBD Delta Control experiment.

OVODAN BIOTECH

OVODAN BIOTECH A/S
Havnegade 36 · DK-5000 Odense C

T +45 6611 1732
E: customerservice@ovodanbiotech.com
www.ovodanbiotech.com

VAT-no: DK 33 87 02 56

Product Datasheet

Spike-RBD 319-514_HIS recombinant protein

For research use only

Description: *Spike-RBD 319-514_HIS*
Expressed in HEK-cell Expi293F system. Protein carries a poly-his tag at the N-terminus.

Correct sequence confirmed by Mass Spectrometry, where full coverage of the sequence has been obtained.

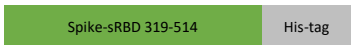

Calculated MW: 27 kDa
Protein migrates as appox. 37 kDa due to glycosylations (See SDS-page beside).

Glycan structures are confirmed, and glycosylation sites identified by Mass Spectrometry of protein samples with and without PNGaseF treatment. (see detailed results below).

Identified glycosylation sites: N42(IT) and N54(AT).

Glycan structures have a combined mass of approx. 6 kDa.

Dimerization percentage < 10%

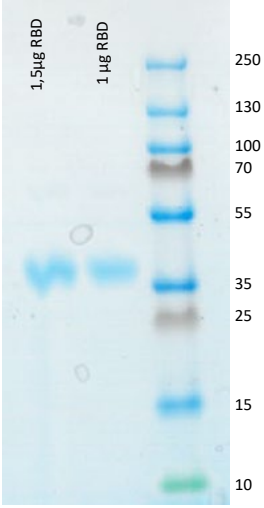

Formulation: In PBS solution pH=7.4

Purification: Immobilized metal affinity chromatography, NiNTA.

Purity: > 95% as determined by SDS-PAGE

Storage: Store at -70°C short term. Avoid freeze thaw cycles.

a THORNICO company

Bioactivity:

ELISA: Specificity towards Human ACE2

Immobilized Human ACE2 1 µg/mL (100µL/well) can bind SARS-CoV-2 Spike RBD 319-514 recombinant protein in a sandwich ELISA setup: ACE2 receptor + RBD recombinant antigen + anti SARS-CoV-2 Spike RBD 319-514 polyclonal IgY + Rabbit anti chicken IgG-HRP.

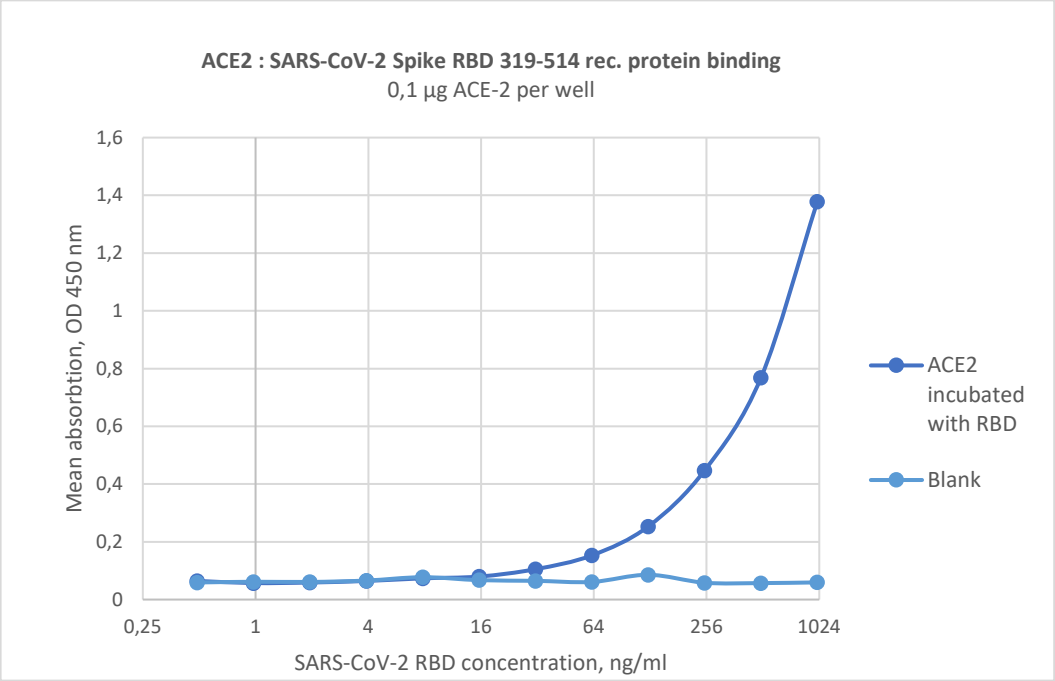

ELISA: High immunogenicity verified by immunization of hens.

IgY shows strong antigenicity. Immobilized SARS-CoV-2 Spike RBD 319-514 recombinant protein at 1 µg/mL (100µL/well) binds chicken anti- SARS-CoV-2 Spike RBD 319-514 with a linear range between 64 to 256 ng/mL antibody added over fixed antigen concertation coated on the well. Starting concentration of antibody normalized to 1 µg/mL.

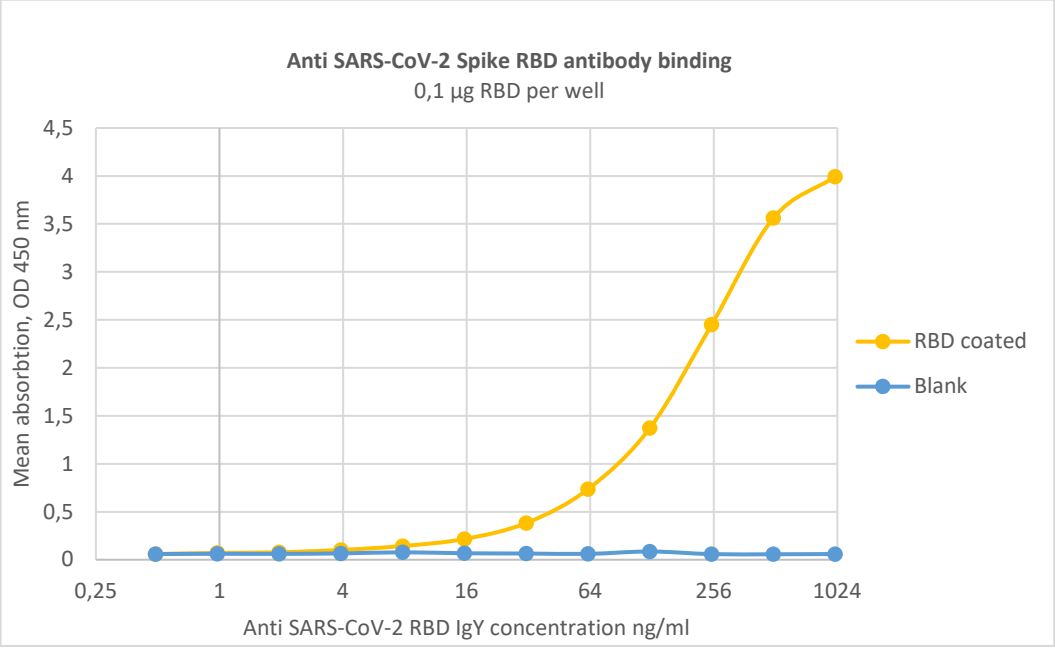

Mass Spectrometry analysis:

The samples have been treated with trypsin for 1h at 57°C (Tryp_CoV_2) or trypsin for 1h at 57°C followed by PNGaseF for 1h at 37°C (Tryp_PNGaseF_CoV_2). Comparison of samples provides knowledge of the glycosylation sites and sequence. Samples analyzed using Thermo Scientific™ Exploris™ 480 Mass Spectrometer.

N42(IT) and N54(AT) have been found to contain glycan structures.

Without PNGaseF

```
MGILPSPGMP ALLSLVSLLS VLLMGCVAFR VQPTESIVRF PNITNLCPFG EVFNATRFAS  60
VYAWNRKRIS NCVADYSVLY NSASFSTFKC YGVSPTKLND LCFTNVYADS FVIRGDEVRQ  120
IAPGQTGKIA DYNYKLPDDF TGCVIAWNSN NLDSKVGGNY NYLYRLFRKS NLKPFERDIS  180
TEIYQAGSTP CNGVEGFNCY FPLQSYGFQP TNGVGYQPYR VVVLSFELLH APATVCGPKK  240
STNLVKNKCV NFGHHHHHHH     260
```

Coverage: 214/260 82.31% own|Spike1|Spike-sRBD 319-514_tyrPho-sig

With PNGaseF

```
MGILPSPGMP ALLSLVSLLS VLLMGCVAFR VQPTESIVRF PNITNLCPFG EVFNATRFAS  60
VYAWNRKRIS NCVADYSVLY NSASFSTFKC YGVSPTKLND LCFTNVYADS FVIRGDEVRQ  120
IAPGQTGKIA DYNYKLPDDF TGCVIAWNSN NLDSKVGGNY NYLYRLFRKS NLKPFERDIS  180
TEIYQAGSTP CNGVEGFNCY FPLQSYGFQP TNGVGYQPYR VVVLSFELLH APATVCGPKK  240
STNLVKNKCV NFGHHHHHHH     260
```

Coverage: 232/260 89.23% own|Spike1|Spike-sRBD 319-514_tyrPho-sig

OVODAN BIOTECH

OVODAN BIOTECH A/S
Havnegade 36 · DK-5000 Odense C

T +45 6611 1732
E: customerservice@ovodanbiotech.com
www.ovodanbiotech.com

VAT-no: DK 33 87 02 56

Product Datasheet

Cat. No: OBA0105

SARS CoV-2 Spike-RBD 319-541 recombinant protein,
Variant of the B1617-2 lineage

For research use only

Description: *SARS-CoV-2 Spike-RBD 319-541 variant B1617-2 (K417N, L452R, T478K)*
Expressed in HEK-cell Expi293F system. Protein carries a poly-his tag at the N-terminus.

Correct sequence confirmed by Mass Spectrometry, where full coverage of the sequence has been obtained.

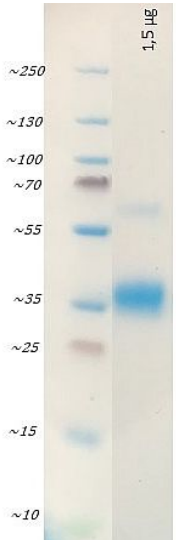

Calculated MW: 27 kDa
Protein migrates as appox. 37 kDa due to glycosylations (See SDS-page beside).

Glycan structures are confirmed, and glycosylation sites identified by Mass Spectrometry of protein samples with and without PNGaseF treatment. (see detailed results below).

Identified glycosylation sites: N42(IT) and N54(AT).

Glycan structures have a combined mass of approx. 6 kDa.

Dimerization percentage < 10%

Formulation: In PBS solution pH=7.4

Purification: Immobilized metal affinity chromatography, NiNTA.

Purity: > 95% as determined by SDS-PAGE

Storage: Store at -70°C short term. Avoid freeze thaw cycles.

a THORNICO company

Bioactivity:

ELISA: High immunogenicity verified by immunization of hens.

The antigen shows strong antigenicity. Immobilized SARS-CoV-2 Spike RBD 319-541 B1617-2 recombinant protein at 1 µg/mL (100µL/well) binds chicken anti- SARS-CoV-2 Spike RBD 319-541 with a linear range between 16 to 1024 ng/mL antibody added over fixed antigen concertation coated on the well. Starting concentration of antibody normalized to 1 µg/mL.

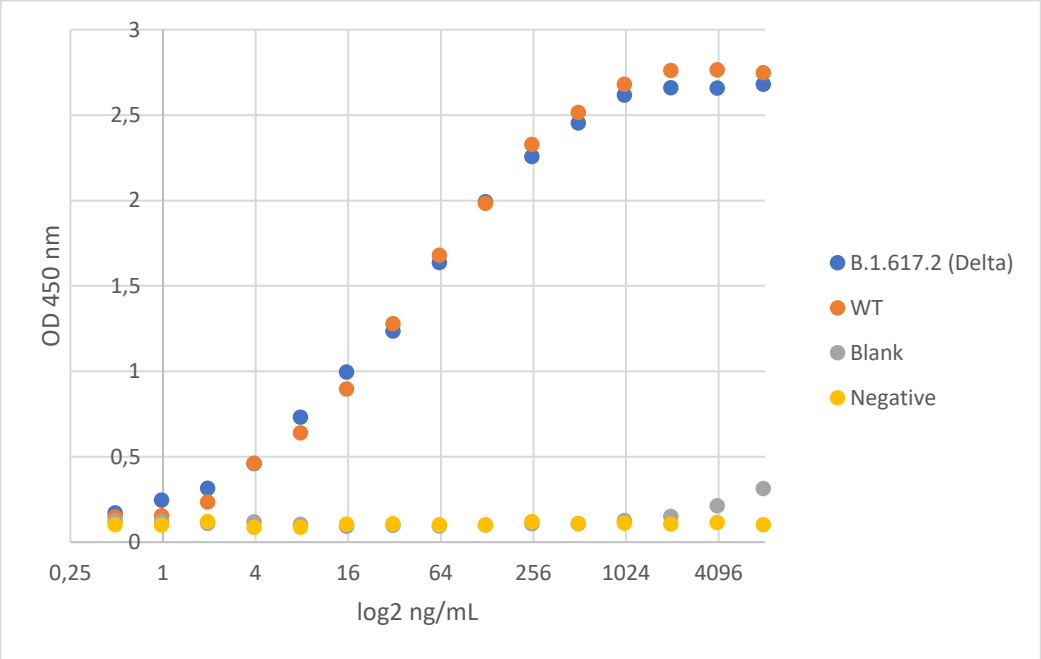

Mass Spectrometry analysis:

The sequence for the variant has been confirmed by mass spectrometry analysis.
Calculated coverage without signal peptide is 92.2%. The missing peptide is caused by glycosylation's on NIT and/or NAT. The one region mutated in this variant is covered showing that the expressed protein matches the B.1617-2 variant amino acid sequence.